



Thermally induced structural changes of intrinsically disordered small heat shock protein Hsp22

Alexey S. Kazakov^a, Denis I. Markov^a, Nikolai B. Gusev^b, Dmitrii I. Levitsky^{a,c,*}

^a A. N. Bach Institute of Biochemistry, Russian Academy of Sciences, Leninsky Pros. 33, 119071 Moscow, Russia

^b Department of Biochemistry, School of Biology, Moscow State University, Russia

^c A. N. Belozersky Institute of Physico-Chemical Biology, Moscow State University, Russia

ARTICLE INFO

Article history:

Received 6 June 2009

Received in revised form 31 August 2009

Accepted 5 September 2009

Available online 12 September 2009

Keywords:

Small heat shock proteins

Intrinsically disordered proteins

Thermal unfolding

Downhill folding

Differential scanning calorimetry

Tryptophan fluorescence

ABSTRACT

We applied different methods (differential scanning calorimetry, circular dichroism, Fourier transform infrared spectroscopy, and intrinsic fluorescence) to investigate the thermal-induced changes in the structure of small heat shock protein Hsp22. It has been shown that this protein undergoes thermal-induced unfolding that occurs within a very broad temperature range (from 27 °C to 80 °C and above), and this is accompanied by complete disappearance of α -helices, significant decrease in β -sheets content, and by pronounced changes in the intrinsic fluorescence. The results confirm predictions that Hsp22 belongs to the family of intrinsically disordered proteins (IDP) with certain parts of its molecule (presumably, in the α -crystallin domain) retaining folded structure and undergoing reversible thermal unfolding. The results are also discussed in terms of downhill folding scenario.

© 2009 Elsevier B.V. All rights reserved.

1. Introduction

Small heat shock proteins (sHsp) play an important role in protecting the cell from various unfavorable conditions [1]. sHsp comprise a large and diverse family of proteins with molecular masses from 12 to 43 kDa. The members of this protein family share so-called α -crystallin domain, consisting of 80–100 amino acid residues, which is located in the C-terminal part of the protein, whereas the N-terminal part differs in sequence and length. *In vitro*, sHsp act as molecular chaperones in preventing denatured proteins from irreversible aggregation [1–3].

A recently described protein with apparent molecular mass of 22 kDa (Hsp22, also denoted as HspB8 or H11 kinase) shares structural properties typical to all members of the family of sHsp [4]. Hsp22 possesses chaperone-like activity [5,6] and appears to be involved in the regulation of many processes such as proliferation, myocardium hypertrophy and apoptosis [7,8].

The far-UV CD data [9,10] have indicated that human Hsp22 contains about 36% of β -sheets, about 5% of α -helices, and about 58% of turns and unordered structures. These data agree with prediction of the secondary structure [6], and together with the results on extra high susceptibility of

Hsp22 to proteolysis [10] indicate that Hsp22 has a predominantly unordered structure. According to the predictions of a structural disorder, it was assumed that Hsp22 belongs to the growing family of intrinsically disordered proteins (IDP), although some parts of its molecule are more or less ordered (residues 90–120 and 140–170 in the α -crystallin domain) [10]. The proteins of the IDP family are characterized by complete or partial lack of folded tertiary structure under physiological conditions *in vitro* [11,12]. Therefore, one of the common features of these proteins is the absence of cooperative thermal transitions on their melting curves [11–14].

In this study, we applied different techniques to investigate structural changes that occur in the Hsp22 molecule upon heating. In good agreement with the earlier made predictions [10], our results indicate that Hsp22 belongs to the IDPs family, although some parts of its molecule (presumably, in the α -crystallin domain) demonstrate thermal unfolding within a wide temperature range. The results of the thermal unfolding of Hsp22 are also discussed in terms of downhill folding scenario.

2. Materials and methods

2.1. Expression and purification of small heat shock proteins (sHsp)

Recombinant human Hsp22 and its K141E mutant were expressed in *E. coli* BL21-DE3 strain and purified by two successive chromatographic steps consisting of hydrophobic chromatography on Phenyl-Sepharose and size-exclusion chromatography on Sephacryl S100 as described earlier [5,9,10]. Hsp27-3D (recombinant human Hsp27 with

Abbreviations: CD, circular dichroism; DSC, differential scanning calorimetry; FTIR, Fourier transform infrared spectroscopy; Hsp22, recombinant human small heat shock protein with apparent molecular mass 22 kDa; IDP, intrinsically disordered proteins; β -ME, β -mercaptoethanol; sHsp, small heat shock protein(s).

* Corresponding author. A. N. Bach Institute of Biochemistry, Russian Academy of Sciences, Leninsky Pros. 33, 119071 Moscow, Russia. Tel.: +7 495 952 1384; fax: +7 495 954 2732.

E-mail address: Levitsky@inbi.ras.ru (D.I. Levitsky).

mutations S15D, S78D and S82D mimicking the naturally occurring phosphorylation) was obtained as described earlier [15,16].

2.2. Intrinsic fluorescence

Fluorescence studies were performed on a Cary Eclipse spectrofluorimeter (Varian) equipped with a Peltier-controlled cell holder and thermoprobes. Intrinsic tryptophan fluorescence was measured at two different Hsp22 concentrations (0.1 and 0.6 mg/ml) in 50 mM Na-phosphate buffer, pH 7.5, containing 150 mM NaCl and 5 mM β -ME. Fluorescence was excited at 297 nm (slit width 5 nm) and recorded in the range of 300–400 nm (slit width 2.5 nm). Correction for inner filter effect at high protein concentration was made using the formula

$$F_{\text{cor}} = F_{\text{obs}} * \text{antilog}[(A_{\text{ex}} + A_{\text{em}}) / 2]$$

where A_{ex} and A_{em} are the absorbance values measured on a Cary 100 spectrophotometer (Varian) at the excitation and emission wavelength, respectively [17]. Spectrofluorimetric temperature scans were performed stepwise allowing the sample to equilibrate at each temperature. The average heating rate was 1 °C/min. The position and form of the fluorescence spectra were characterized by the parameter $A = I_{320}/I_{365}$, where I_{320} and I_{365} are fluorescence intensities at $\lambda_{\text{em}} = 320$ and 365 nm, respectively [18–20]. In order to determine the fraction of conversion of the native form of the protein to its unfolded state (parameter α) we used the fluorescence phase plots (the dependence of fluorescence intensity at 320 nm on the intensity of fluorescence at 365 nm obtained at different temperatures) [21].

2.3. CD spectroscopy

Far-UV CD spectra of Hsp22 (1.2 mg/ml) were recorded on Chirascan Circular Dichroism Spectrometer (Applied Photophysics) in 0.02 cm cells at different temperatures with a constant heating rate of 1 °C/min. Each CD plot was an average of 3 accumulated scans. Plots were baseline corrected for buffer (50 mM Na-phosphate, pH 7.5, containing 150 mM NaCl and 2 mM DTT).

2.4. Differential scanning calorimetry (DSC)

DSC experiments were performed on a DASM-4M differential scanning microcalorimeter (Institute for Biological Instrumentation RAS, Pushchino, Russia) at a 1 °C/min heating rate in 50 mM Na-phosphate buffer, pH 7.5, containing 150 mM NaCl and 2 mM β -ME. Protein concentrations were 0.6–1.2 mg/ml. The reversibility of the heat sorption curves was assessed by reheating of the sample immediately after cooling from the previous scan. The DSC scan obtained from the first heating of the β -ME-containing sample was omitted as this heating was specially destined to reduce SH-groups of the protein and to prevent disulfide cross-linking, and all following scans (up to five) were identical. The heat sorption curves were baseline corrected in two different ways: either by subtracting a scan with buffer in both cells, or by using a special DSC approach, which was successfully applied in earlier studies to reveal small and low-cooperative thermal transitions in non-muscle tropomyosins [22]. Briefly, DSC measurements were performed not only in the usual way, when the protein was placed into the sample cell and the buffer was placed into the reference cell, but also *vice versa*, with the same protein sample in the reference cell and the buffer in the sample cell. This inverted curve was then subtracted from the curve obtained by the usual way. The above DSC approach allows us to subtract the instrumental baseline with very high precision [22]. Protein-specific heat capacity (C_p) was calculated as described by Privalov and Potekhin [23], and C_p of fully unfolded Hsp22 was estimated according to Hackel et al. [24].

2.5. Fourier transform infrared spectroscopy (FTIR)

FTIR spectra were recorded on a Tensor 27 FTIR spectrophotometer (Bruker) equipped with BioATR II cell with the silicon crystal. Approximately 20 μ l of Hsp22 (7 mg/ml) in 50 mM Na-phosphate buffer, pH 7.5, containing 150 mM NaCl and 5 mM β -ME, was applied on the crystal. The spectra were recorded at different temperatures using a resolution of 4 cm^{-1} and 500 accumulations. Secondary structure content was determined by using OPUS 6.0 software (Bruker) from curve fitting to spectra (amide I region) deconvoluted using second derivatives to identify component band positions. The data were automatically corrected for water (liquid and vapor) and CO_2 components by the OPUS 6.0.

2.6. Chaperone-like activity

The chaperone-like activity of Hsp22 and its K141E mutant was determined by their ability to prevent heat-induced aggregation of F-actin as described previously for experiments with small heat shock protein Hsp27 and its 3D mutant [25,26]. Thermally induced aggregation of F-actin was measured by light scattering on a Cary Eclipse spectrofluorimeter (Varian) equipped with a Peltier-controlled cell holder and thermoprobes. F-actin in the absence or in the presence of sHsp was heated at a constant rate of 1 °C/min from 30 °C up to 90 °C. The light scattering at 350 nm was measured with excitation and emission slits of 2.5 and 1.5 nm, respectively.

3. Results

3.1. Temperature-induced changes in the intrinsic fluorescence of Hsp22

Hsp22 contains four Trp residues (Fig. 1A) and at room temperature the Trp fluorescence spectrum of Hsp22 is characterized by the red-shifted maximum ($\lambda_{\text{max}} = 341$ nm) (Fig. 1B). It is known that a Trp emission maximum is highly dependent on the polarity of its environment: a Trp residue in a non-polar environment (i.e., buried inside a protein), has an emission maximum close to 320 nm, while in a polar environment (i.e., solvent-exposed) it has the maximum close to 350 nm. Therefore the red-shifted maximum of fluorescence indicates that a large portion of Hsp22 Trp residues is solvent-exposed. This conclusion agrees with the prediction of disordered regions in Hsp22 [10] indicating that three Trp residues are located in presumably unordered regions and only Trp96 is located in a more or less ordered region (residues 90–120 of α -crystallin domain). If this prediction is correct, we might suppose that at least for one Trp residue the temperature-induced unfolding will be accompanied by more or less cooperative changes of fluorescence parameters.

Upon heating from 20 °C to 80 °C, the Trp fluorescence spectrum of Hsp22 demonstrates significant red shift of its emission maximum from 341 nm up to 351 nm (Fig. 1B). An increase of the λ_{max} value occurs within a wide temperature range, from 30 °C to 80 °C, and it is accompanied by a decrease of parameter $A = I_{320}/I_{365}$, with a mid-transition temperature of 57 °C for both curves (Fig. 1C). Both these parameters cannot be used for quantitative determination of the fraction of conversion from native to denatured state. However, both these parameters indicate that there is more or less co-operative transition at about 57 °C. It is worthwhile to mention that this transition was completely reversible and that the mid-transition temperature was not dependent on the protein concentration in the range of 0.1–0.6 mg/ml (Fig. 1C).

For quantitative analysis of the thermal-induced unfolding of Hsp22 we applied the method of parametric plots [21]. Fig. 2 shows the dependence of fluorescence intensity at 320 nm on the intensity of fluorescence at 365 nm obtained at different temperatures. In this case, the fluorescence intensities at 320 and 365 nm were used as independent extensive characteristics (as opposed to intensive characteristics such as parameter A and λ_{max}), and the temperature was taken as a parameter.

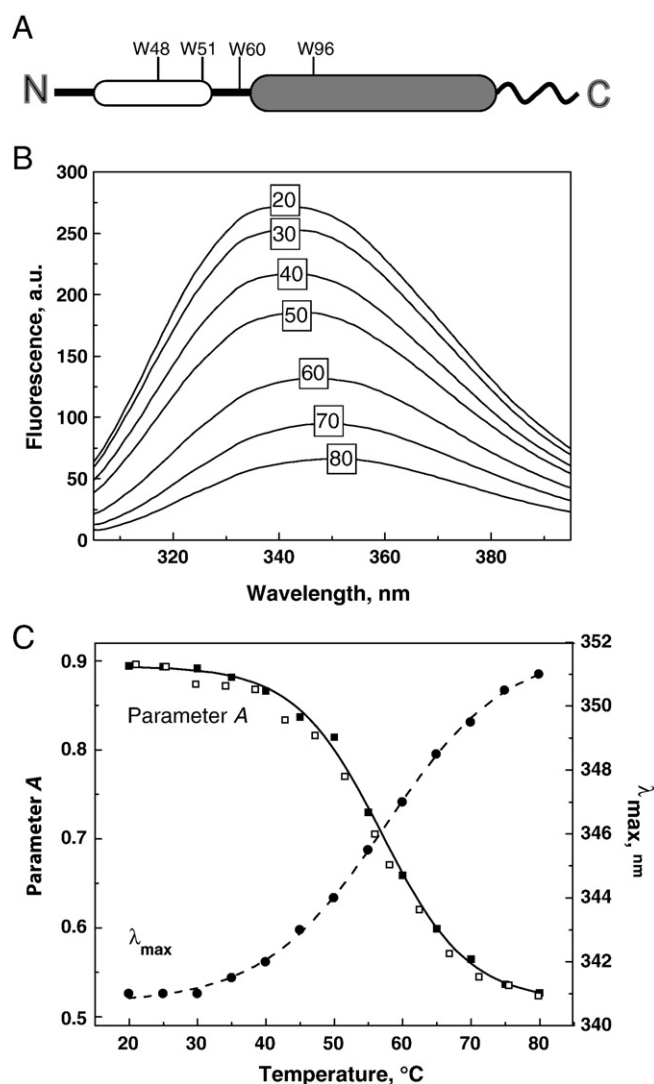


Fig. 1. (A) Localization of four Trp residues in Hsp22 primary structure. The α -crystallin domain is shown in dark gray and variable N-terminal part in white. (B) Intrinsic Trp fluorescence spectra as measured during heating of Hsp22 from 20 °C to 80 °C (the temperature values are indicated in squares for each spectrum). (C) Temperature-induced changes of the Hsp22 intrinsic fluorescence measured by the changes of the spectrum position (λ_{\max}) and of the value of parameter $A = I_{320}/I_{365}$. Filled and empty symbols on the curve of parameter A correspond to the data obtained at Hsp22 concentration equal to 0.1 and 0.6 mg/ml respectively.

The linear parts of the plot extrapolated to zero correspond to the common thermal fluorescence quenching without any change in the protein structure, and the curve between these lines corresponds to thermal transition in the protein structure. The lines indicated as N and U (native and unfolded states of Trp-containing regions, respectively) represent extrapolations of the linear parts of the phase plot to the thermal transition region. This approach allowed quantitative determination of the so-called parameter α , the fraction of conversion from native to denatured state [21]. The temperature dependence of this parameter (Fig. 3) clearly demonstrates that Hsp22 undergoes thermal unfolding within a temperature range from 39 °C to 74 °C, showing cooperative thermal transition with a mid-point temperature of 58 °C. Cooperative character of this transition even permits estimation of Van't Hoff enthalpy of this transition (Fig. 3). It is important to note that mid-point of this transition (58 °C) is very similar to the mid-transition temperature of 57 °C obtained by measuring intensive characteristics, λ_{\max} and parameter A (Fig. 1C).

Previous studies have shown that mutation K141E induces destabilization of Hsp22 structure increasing susceptibility of Hsp22

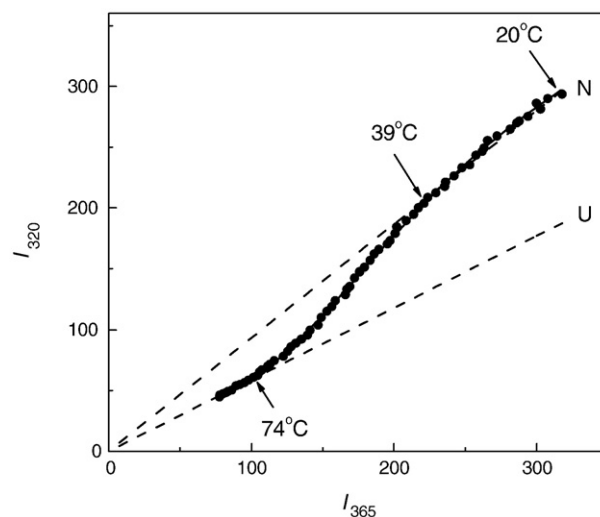


Fig. 2. Parametric dependences of fluorescence intensity at 320 and 365 nm, characterizing the temperature-induced unfolding of Hsp22. The variable parameter is the temperature. Fluorescence characteristics of native (N) and completely unfolded (U) Trp-containing regions of Hsp22 are indicated. Values of fluorescence intensities are expressed in relative units.

to trypsinolysis [9]. In good agreement with these data, we found that mutation K141E strongly decreases the thermal stability of Hsp22 as measured by Trp fluorescence. This mutation shifts the curve of the temperature dependence of parameter α by ~ 7 °C to the lower temperature, from 58 °C to 51 °C (Fig. 3).

3.2. DSC studies of the thermal unfolding of Hsp22

DSC results show that Hsp22 undergoes thermal-induced unfolding (Fig. 4). At low temperature the specific heat capacity (C_p) of Hsp22 significantly exceeds the heat capacity expected for a globular protein having stable, fully folded structure and the same molecular mass as Hsp22, as calculated according to Privalov and co-authors

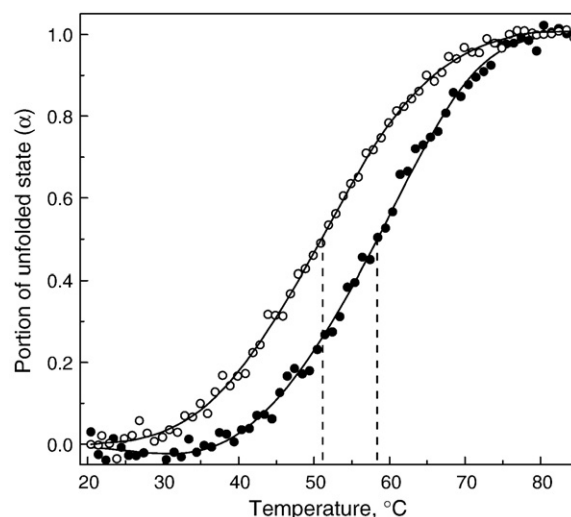


Fig. 3. Temperature-induced changes in the fraction of unfolded state (α) for the wild type Hsp22 (filled symbols) and its K141E mutant (empty symbols). The fractions of unfolded state were calculated from parametric dependences of fluorescence intensity at 320 and 365 nm. Vertical dotted lines indicate the temperatures of half-maximum changes in parameter α (58 °C for wild type Hsp22 and 51 °C for its K141E mutant). The values of Van't Hoff enthalpy estimated for these transitions of wild type Hsp22 and its K141E mutant were equal to 150 and 130 kJ/mol, respectively.

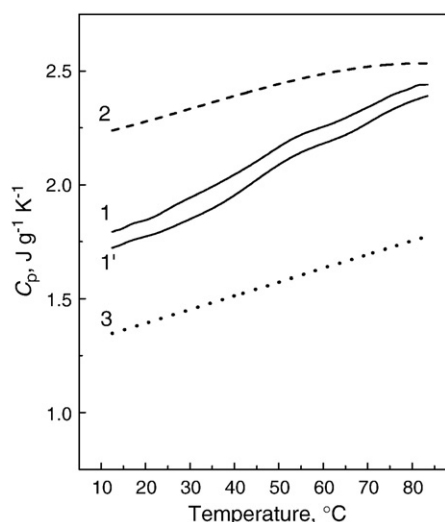


Fig. 4. The thermal-induced unfolding of Hsp22 monitored by DSC. Solid curves 1 and 1' represent the temperature dependence of specific heat capacity of Hsp22 estimated from two independent DSC experiments. Dashed curve 2 corresponds to the heat capacity of fully unfolded Hsp22, as estimated according to Hackel et al. [24]. Dotted line 3 represents the expected heat capacity of a globular protein having a stable and rigid structure: it was calculated according to Privalov and co-authors [27,28], using the molecular mass of Hsp22. The absolute error of specific heat capacity (C_p) did not exceed $\pm 0.1 \text{ J g}^{-1} \text{ K}^{-1}$.

[27,28]. At the same time at room temperature, the C_p values of Hsp22 are less than the values of fully unfolded Hsp22, as estimated according to Hackel et al. [24]. These DSC data unambiguously indicate that at low temperature a significant portion of the Hsp22 molecule lacks rigid tertiary structure and therefore possesses properties of intrinsically disordered proteins. However, under these conditions Hsp22 is not completely unfolded. Upon heating, the heat capacity of Hsp22 steeply increases, starting from 27 °C, and it becomes close to the C_p values of fully unfolded Hsp22 above 80 °C (Fig. 4). This indicates that the largest part of the Hsp22 molecule is disordered and lacks rigid tertiary structure, and therefore its thermal unfolding is expressed as a continuous transition within a wide temperature range. Such type of transition was recently observed by DSC for intrinsically disordered apo-parvalbumin [29] and for artificial miniprotein FSD-1ss [30]. It should be noted, however, that in the last case the thermally-induced unfolding started from completely folded state and reached completely unfolded state at high temperature [30].

Although we were unable to detect large sorption peaks on the curve of temperature dependence of specific heat capacity, careful investigation of this curve indicates the presence of a small peak with an apparent half-transition temperature of about 52–54 °C (Fig. 4). This temperature is similar (although slightly lower) to that determined for half-maximal transition of the thermal unfolding of Hsp22 obtained from fluorescence experiments (Figs. 1C, 3) and might correspond to the melting of certain parts of α -crystallin domain, probably containing Trp96. It is worthwhile to mention that the thermal-induced unfolding of Hsp22 was independent of protein concentration in the range of 0.6–1.2 mg/ml and was completely reversible, as DSC curves of the same Hsp22 sample can be repeated many times, without any changes, during re-heatings of the sample.

3.3. Temperature-induced changes in the secondary structure of Hsp22

Far-UV CD and FTIR were used to analyze the thermally-induced changes in Hsp22 secondary structure. Fig. 5A represents the far-UV CD spectra of Hsp22 measured at different temperatures. At 20 °C, the protein possesses a far-UV CD spectrum typical of an essentially unfolded polypeptide chain [13,14,31]. The spectrum has an intense

minimum in the vicinity of 200 nm, with the absence of characteristic bands in the range of 210–230 nm. It is noteworthy that the ratio of ellipticity at 222 nm ($[\theta]_{222} = -2140 \text{ deg cm}^2 \text{ dmol}^{-1}$) to that at 200 nm ($[\theta]_{200} = -5756 \text{ deg cm}^2 \text{ dmol}^{-1}$) on the CD spectrum of Hsp22 is equal to 0.37. According to “double wavelength” plot, $[\theta]_{222}$ vs $[\theta]_{200}$, proposed by Uversky [13], the CD spectrum of Hsp22 roughly,

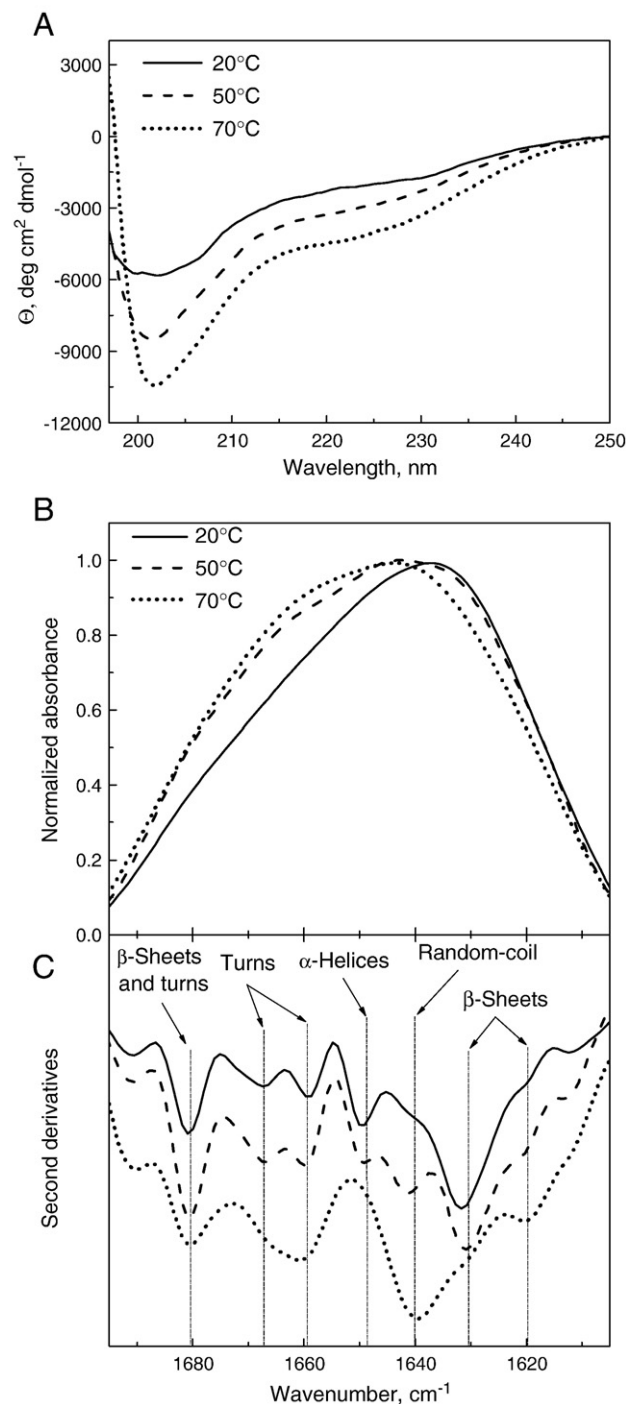


Fig. 5. Thermal-induced changes in the secondary structure of Hsp22, as measured by CD (A) and FTIR (B,C). The far-UV CD spectra (A) and normalized FTIR spectra of the amide I region (B) were measured at 20 °C (solid curves), 50 °C (dashed curves), and 70 °C (dotted curves). (C) Normalized second derivatives of the corresponding FTIR spectra shown in (B). The curves are shifted for clarity of presentation. The vertical dashed-and-dotted lines indicate the peaks assigned to β -sheets (the peaks at 1620 and 1631 cm^{-1}), α -helices (the peak around 1651 cm^{-1}), disordered random-coil structure (the broad peak around 1641 cm^{-1}), and turns (peaks at 1660, 1667 and 1681 cm^{-1}).

but not entirely, corresponds to that of a protein in the pre-molten-globule-like state. These CD data indicate that the structure of Hsp22 is more ordered than that typical for proteins in the pre-molten-globule-like state. As the temperature is increased, the spectrum changes: the minimum becomes more intense, and the negative intensity of the spectrum around 222 nm increases (Fig. 5A). At 70 °C, the ratio $[\theta]_{222}/[\theta]_{200}$ becomes equal to 0.47 ($[\theta]_{222} = -4353 \text{ deg cm}^2 \text{ dmol}^{-1}$ and $[\theta]_{200} = -9207 \text{ deg cm}^2 \text{ dmol}^{-1}$). This means, according to the “double wavelength” plot [13], that under these conditions Hsp22 reaches the pre-molten-globule-like state. It is worthwhile mentioning that similar temperature-induced changes of the far-UV CD spectra are typical for many IDPs [14] and that in the case of Hsp22 these changes of the secondary structure were completely reversible. The molar ellipticities at 200, 209 and 222 nm were linearly dependent on the temperature and we were unable to observe any pronounced thermal transitions (data not shown).

We also applied the FTIR method to analyze the temperature-induced changes in the secondary structure of Hsp22. We have used this method since FTIR provides a more reliable determination of the β -structure than the CD spectroscopy [32]. Fig. 5B shows the FTIR (amide I region) spectra of Hsp22 measured at 20 °C, 50 °C, and 70 °C. An increase in temperature leads to significant spectral changes, which are reflected in the shift of the maximum from 1637 cm^{-1} to 1644 cm^{-1} and the appearance of a shoulder in the vicinity of 1660 cm^{-1} (Fig. 5B). These changes of the FTIR spectrum are due to the changes in the intensity of certain peaks corresponding to different elements of the secondary structure. These peaks were assigned by using second derivative of FTIR spectra (Fig. 5C). Independent of the temperature we detected seven negative peaks around $1621, 1631, 1641, 1651, 1661, 1667$, and 1681 cm^{-1} on the second derivative of FTIR spectra. These peaks correspond to β -sheets, α -helices, turns, and random-coil disordered structure, as indicated on Fig. 5C. Deconvolution of the FTIR spectra based on the assignment of corresponding peaks and performed by OPUS 6.0 software (Bruker) provides information on the secondary structure of Hsp22 at different temperatures. The data of FTIR indicate that at 20 °C Hsp22 contains about 33% of β -sheets, about 12% of α -helices, about 34% of turns, and about 21% disordered random-coil structures. This estimation correlates well with the corresponding data obtained earlier by CD spectroscopy [9]. According to predictions, almost all β -strands of Hsp22 are located in the α -crystallin domain, while α -helices are mainly localized in the N-terminal part of the molecule [10]. Increase of the temperature up to 50 °C was accompanied by slight decrease of the percentage of α -helices (1650 cm^{-1}) and β -sheets (1620 and 1630 cm^{-1}) and increase of the random-coil and turns ($1642, 1660, 1667$, and 1681 cm^{-1}) in the structure of Hsp22. As the temperature is further increased up to 70 °C, the peak of α -helices completely disappears and the content of β -sheets decreases from 33 down to 18%. At the same time, the percentage of turns and disordered random-coil structures increases up to 45% and 37%, respectively. These data indicate that Hsp22 undergoes thermal unfolding that is accompanied by decrease of the ordered and increase of the unordered structure, with the main changes in its secondary structure occurring above 50 °C.

3.4. Effect of Hsp22 and its K141E mutant on heat-induced aggregation of F-actin

We studied the chaperone-like activity of Hsp22 and its K141E mutant by determining their ability to prevent aggregation of F-actin induced by its thermal denaturation. This test-system was successfully used in the previous studies to investigate the chaperone-like activity of other recombinant human sHsp [25,26]. In the present work, we used this test-system to investigate the chaperone-like activity of Hsp22 and its K141E mutant in comparison with that of Hsp27-3D (Fig. 6).

F-actin (0.1 mg/ml) was heated at a constant rate of $1 \text{ }^\circ\text{C}/\text{min}$ up to $90 \text{ }^\circ\text{C}$ in the absence or in the presence of the wild type Hsp22, its K141E mutant, or Hsp27-3D at weight ratio of sHsp to actin equal to 1:1. As it was shown earlier by DSC studies, F-actin was fully denatured above $70 \text{ }^\circ\text{C}$ both in the absence and in the presence of sHsp [25]. In the absence of sHsp, thermal denaturation of F-actin was accompanied by a strong increase in light scattering (Fig. 6, curve 1). Hsp27-3D effectively prevented aggregation of denatured actin and shifted the aggregation curve to the higher temperatures, above $80 \text{ }^\circ\text{C}$ (Fig. 6, curve 4). It is worthwhile to mention that, in the presence of Hsp27-3D, F-actin started to aggregate at about $70 \text{ }^\circ\text{C}$, i.e. the temperature, at which the thermal unfolding of Hsp27-3D occurred [25]. Hsp22 also retarded the thermal-induced aggregation of F-actin, however its chaperone-like activity was less pronounced than in the case with Hsp27-3D. For instance, in the presence of Hsp22, the increase of light scattering started below $60 \text{ }^\circ\text{C}$, and the aggregation curve was shifted by $10\text{--}12 \text{ }^\circ\text{C}$ to the higher temperature in comparison with the corresponding curve for isolated F-actin (Fig. 6, curve 2). K141E mutant of Hsp22 was less effective than the wild type protein in retarding thermal-induced aggregation of F-actin and the aggregation curve was shifted by only $5\text{--}6 \text{ }^\circ\text{C}$ to the higher temperature in comparison with the curve for isolated F-actin (Fig. 6, curve 3).

The efficiency of prevention of thermal-induced aggregation correlates with thermal stability of sHsp. For instance, Hsp27-3D that unfolds at temperature higher than $70 \text{ }^\circ\text{C}$ [25,33,34] is the most effective, whereas the wild type Hsp22 and especially its K141E mutant undergoing thermal unfolding at about 58 and $51 \text{ }^\circ\text{C}$ are less effective in retarding F-actin aggregation that starts at about $55 \text{ }^\circ\text{C}$ (Fig. 6).

4. Discussion

The results presented here indicate that Hsp22 belongs to the IDPs family. The red-shifted fluorescence spectrum (Fig. 1B) indicates that the largest part of Trp residues of Hsp22 is solvent-exposed. This conclusion agrees with the earlier made prediction [10] indicating that among four Trp residues of Hsp22 the only one, namely Trp96, is located in one of the two partially ordered parts (residues $90\text{--}120$ and $140\text{--}170$) in the α -crystallin domain of Hsp22. The heating is accompanied by the changes in fluorescence parameters with mid-transition temperature of about $58 \text{ }^\circ\text{C}$ and by significant decrease in

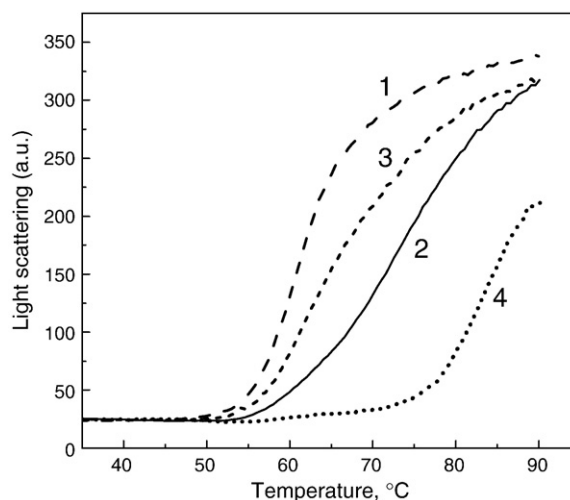


Fig. 6. Effects of Hsp22, its K141E mutant, and Hsp27-3D on the heat-induced aggregation of F-actin. F-actin (0.1 mg/ml) was heated at a constant rate of $1 \text{ }^\circ\text{C}/\text{min}$ in the absence (curve 1) or in the presence of wild type Hsp22 (curve 2), its K141E mutant (curve 3) or Hsp27-3D (curve 4), and aggregation was followed by light scattering at 350 nm. The concentration of all sHsp was equal to 0.1 mg/ml.

the content of β -sheets. These changes probably correspond to the thermal-induced unfolding of certain parts of α -crystallin domain containing Trp96. Mutation K141E destabilizes the α -crystallin domain [10] and probably therefore thermal-induced changes of the fluorescent parameters of K141E mutant of Hsp22 occur at lower temperature than the corresponding changes of the wild type protein (Fig. 3).

DSC results have shown that the thermal unfolding of Hsp22 occurs within a very broad temperature range, and it is characterized by the absence of a pronounced excess heat sorption peak (Fig. 4). In this respect, Hsp22 is quite different from all other mammalian sHsp studied by DSC, e.g. Hsp27 and α -crystallin, which demonstrated cooperative thermal transitions at $\sim 70^\circ\text{C}$ for Hsp27 [25,33,34] and at $\sim 60^\circ\text{C}$ for α -crystallin [35,36]. This indicates that Hsp22, in contrast with Hsp27 and α -crystallin, lacks rigid tertiary structure. This can be due to some peculiarities of Hsp22 primary structure. For instance, the position that is occupied by $\beta 2$ -strand in the structure of other human sHsp is presented in Hsp22 by the sequence TPTTFFP that prevents formation of the β -strand [10]. This might induce destabilization of the whole α -crystallin domain. Moreover, the $\beta 2$ -strand seems to play an important role in the intersubunit interaction of different sHsp [37] and therefore the lack of this strand might impede formation of stable dimers of Hsp22. It seems likely that formation of stable dimers, provided by interaction of α -crystallin domains of two neighboring monomers [1,3,37], plays an important role in the stabilization of the sHsp molecule, and this may explain, at least partly, why Hsp22 is intrinsically disordered. The inability to form stable dimers as well as the absence of conservative I-X-(I/V) sequence in the flexible C-terminal end [37] makes improbable formation of high molecular mass oligomers of Hsp22. Therefore unlike the most other sHsp, Hsp22 is presented only in the form of monomers or small oligomers [4–6,8,9]. All these factors probably lead to further destabilization of the Hsp22 structure.

Intrinsically disordered nature and low stability of the structure affect the chaperone-like activity of Hsp22 measured by heat-induced aggregation of F-actin (Fig. 6). In this respect, it is worthwhile to mention that mutation K141E, which strongly decreases the thermal stability of Hsp22 (Fig. 3), simultaneously decreases its chaperone-like activity (Fig. 6). These data suggest that a relationship may exist between thermal stability and chaperone-like activity of Hsp22, at least with respect to its ability to prevent heat-induced aggregation of F-actin. This might be another explanation why intrinsically disordered Hsp22, which is less thermostable than Hsp27-3D and is unable to form large oligomers, is less effective than Hsp27-3D in preventing thermal-induced aggregation of F-actin. In any case, the stability of tertiary and/or quaternary structure of sHsp appears to be of great importance for their chaperone-like activity.

Thus, our results indicate that Hsp22 belongs to the IDPs family. However, the results of the Hsp22 thermal unfolding can be also considered from another viewpoint, namely in the light of recently described downhill behavior of some proteins. The energy landscape theory predicts that under certain conditions, protein folding can proceed without crossing free energy barriers (the downhill scenario). A characteristic feature of this scenario is the existence of a unique thermodynamic state consisting of an ensemble of conformations that loses structure gradually as protein stability decreases. Therefore, the folding/unfolding process is non-cooperative in this case, and the apparent transition depends on the method probing certain structural properties of the protein as it unfolds. According to the downhill folding/unfolding scenario, various techniques applied to investigate protein unfolding give different characteristics of the thermal transition [38,39]. It seems to us, this is just the case with the thermal unfolding of Hsp22. DSC results have shown a continuous transition without pronounced heat sorption peak, and only very small peak at $52\text{--}54^\circ\text{C}$ was observed (Fig. 4). Similarly, CD experiments on the Hsp22 thermal unfolding did not reveal any pronounced thermal

transitions (data not shown). On the other hand, the results of fluorescence studies clearly demonstrated the cooperative thermal transition at 58°C , for which it was even possible to estimate the Van't Hoff enthalpy (Fig. 3). Our data agree with the main criteria of the downhill folding scenario [38,39]. Such type of behavior was earlier predicted from simulation analysis of the thermal unfolding of a model protein [39], and our experimental data confirm this prediction.

In conclusion, it should be noted that both points of view, i.e. thermal unfolding of Hsp22 as IDP or as a downhill folder, are not in contradiction but supplement each other. Analysis of the thermal unfolding of Hsp22 as IDP examines structural traits of the protein, whereas consideration of Hsp22 as a downhill folder allows to clarify its thermodynamic properties.

Acknowledgments

We thank Bruker Ltd. (Moscow) for the help in analysis of FTIR data. This work was supported by the grants from Russian Foundation for Basic Research and by the Program "Molecular and Cell Biology" of the Russian Academy of Sciences.

References

- [1] M. Haslbeck, T. Franzmann, D. Weinfurter, J. Buchner, Some like it hot: the structure and function of small heat-shock proteins, *Nat. Struct. Mol. Biol.* 12 (2005) 842–846.
- [2] M. Haslbeck, sHsps and their role in the chaperone network, *Cell Mol. Life Sci.* 59 (2002) 1649–1657.
- [3] N.B. Gusev, N.V. Bogatcheva, S.B. Marston, Structure and properties of small heat shock proteins (sHsp) and their interaction with cytoskeleton proteins, *Biochemistry (Moscow)* 67 (2002) 511–519.
- [4] R. Benndorf, X. Sun, R.R. Gilmont, K.J. Biederman, M.P. Molloy, C.W. Goodmurphy, H. Cheng, P.C. Andrews, M.J. Welsh, HSP22, a new member of the small heat shock protein superfamily, interacts with mimic of phosphorylated HSP27 ((3D)HSP27), *J. Biol. Chem.* 276 (2001) 26753–26761.
- [5] M.V. Kim, A.S. Seit-Nebi, S.B. Marston, N.B. Gusev, Some properties of human small heat shock protein Hsp22 (H11 or HspB8), *Biochem. Biophys. Res. Commun.* 315 (2004) 796–801.
- [6] T.K. Chowdary, B. Raman, T. Ramakrishna, C.M. Rao, Mammalian Hsp22 is a heat-inducible small heat-shock protein with chaperone-like activity, *Biochem. J.* 381 (2004) 379–387.
- [7] M. Hase, C. Depre, S.F. Vatner, J. Sadoshima, H11 has dose-dependent and dual hypertrophic and proapoptotic function in cardiac myocytes, *Biochem. J.* 388 (2005) 475–483.
- [8] A.A. Shemetov, A.S. Seit-Nebi, N.B. Gusev, Structure, properties, and functions of the human small heat-shock protein HSP22 (HspB8, H11, E2IG1): a critical review, *J. Neurosci. Res.* 86 (2007) 264–269.
- [9] M.V. Kim, A.S. Kasakov, A.S. Seit-Nebi, S.B. Marston, N.B. Gusev, Structure and properties of K141E mutant of small heat shock protein HSP22 (HspB8, H11) that is expressed in human neuromuscular disorders, *Arch. Biochem. Biophys.* 454 (2006) 32–41.
- [10] A.S. Kasakov, O.V. Bukach, A.S. Seit-Nebi, S.B. Marston, N.B. Gusev, Effect of mutations in the $\beta 5\text{--}\beta 7$ loop on the structure and properties of human small heat shock protein HSP22 (HspB8, H11), *FEBS J.* 274 (2007) 5628–5642.
- [11] P. Tompa, Intrinsically unstructured proteins, *Trends Biochem. Sci.* 27 (2002) 527–533.
- [12] V.N. Uversky, C.J. Oldfield, A.K. Dunker, Showing your ID: intrinsic disorder as an ID for recognition, regulation and cell signaling, *J. Mol. Recognit.* 18 (2005) 343–384.
- [13] V.N. Uversky, Natively unfolded proteins: a point where biology waits for physics, *Protein Sci.* 11 (2002) 739–756.
- [14] V.N. Uversky, What does it mean to be natively unfolded? *Eur. J. Biochem.* 269 (2002) 2–12.
- [15] O.O. Panasenkov, M.V. Kim, S.B. Marston, N.B. Gusev, Interaction of the small heat shock protein with molecular mass 25 kDa (hsp25) with actin, *Eur. J. Biochem.* 270 (2003) 892–901.
- [16] O.V. Bukach, A.S. Seit-Nebi, S.B. Marston, N.B. Gusev, Some properties of human small heat shock protein Hsp20 (HspB6), *Eur. J. Biochem.* 271 (2004) 291–302.
- [17] P.M. Schwarz, J.R. Liggins, R.F. Luduena, β -Tubulin isotypes purified from bovine brain have different relative stabilities, *Biochemistry* 37 (1998) 4687–4692.
- [18] K.K. Turoverov, S.Yu. Khaitlina, G.P. Pinaev, Ultra-violet fluorescence of actin. Determination of native actin content in actin preparations, *FEBS Lett.* 62 (1976) 4–7.
- [19] K.K. Turoverov, I.M. Kuznetsova, Intrinsic fluorescence of actin, *J. Fluoresc.* 13 (2003) 41–57.
- [20] M. Staiano, V. Scognamiglio, M. Rossi, S. D'Auria, O.V. Stepanenko, I.M. Kuznetsova, K.K. Turoverov, Unfolding and refolding of the glutamine-binding protein from *Escherichia coli* and its complex with glutamine induced by guanidine hydrochloride, *Biochemistry* 44 (2005) 5625–5633.

- [21] E.A. Permyakov, W.A. Burstein, Some aspects of studies of thermal transitions in proteins by means of their intrinsic fluorescence, *Biophys. Chem.* 19 (1984) 265–271.
- [22] E. Kremneva, O. Nikolaeva, R. Maytum, A.M. Arutyunyan, S.Yu. Kleimenov, M.A. Geeves, D.I. Levitsky, Thermal unfolding of smooth muscle and nonmuscle tropomyosin α -homodimers with alternatively spliced exons, *FEBS J.* 272 (2006) 588–600.
- [23] P.L. Privalov, S.A. Potekhin, Scanning microcalorimetry in studying temperature-induced changes in proteins, *Methods Enzymol.* 131 (1986) 4–51.
- [24] M. Hackel, H.J. Hinz, G.R. Hedwig, A new set of peptide-based group heat capacities for use in protein stability calculations, *J. Mol. Biol.* 291 (1999) 197–213.
- [25] A.V. Pivovarova, V.V. Mikhailova, I.S. Chernik, N.A. Chebotareva, D.I. Levitsky, N.B. Gusev, Effects of small heat shock proteins on the thermal denaturation and aggregation of F-actin, *Biochem. Biophys. Res. Commun.* 331 (2005) 1548–1553.
- [26] A.V. Pivovarova, N.A. Chebotareva, I.S. Chernik, N.B. Gusev, D.I. Levitsky, Small heat shock protein Hsp27 prevents heat-induced aggregation of F-actin by forming soluble complexes with denatured actin, *FEBS J.* 274 (2007) 5937–5948.
- [27] G.I. Makhatadze, P.L. Privalov, Energetics of protein structure, *Annu. Rev. Protein Chem.* 47 (1995) 307–425.
- [28] A.I. Dragan, P.L. Privalov, Unfolding of a leucine zipper is not a simple two-state transition, *J. Mol. Biol.* 321 (2002) 891–908.
- [29] S.E. Permyakov, A.G. Bakunts, A.I. Denesyuk, E.L. Knyazeva, V.N. Uversky, E.A. Permyakov, Apo-parvalbumin as an intrinsically disordered protein, *Proteins* 72 (2008) 822–836.
- [30] M. Sadqi, E. de Alba, R. Perez-Jimenez, J.M. Sanchez-Ruiz, V. Munoz, A designed protein as experimental model of primordial folding, *Proc. Natl. Acad. Sci. U. S. A.* 106 (2009) 4127–4132.
- [31] V.N. Uversky, J. Li, A.L. Fink, Evidence for a partially folded intermediate in α -synuclein fibril formation, *J. Biol. Chem.* 276 (2001) 10737–10744.
- [32] E. Goormaghtigh, R. Gasper, A. Benard, A. Goldsztein, V. Raussens, Protein secondary structure content in solution, films, and tissues: redundancy and complementarity of the information content in circular dichroism, transmission and ATR FTIR spectra, *Biochim. Biophys. Acta* 1794 (2009) 1332–1343.
- [33] I.V. Dudich, V.P. Zav'yalova, W. Pfeil, M. Gaestel, G.A. Zav'yalova, A.I. Denesyuk, T. Korpela, Dimer structure as a minimum cooperative subunit of small heat-shock proteins, *Biochim. Biophys. Acta* 1253 (1995) 163–168.
- [34] D.I. Markov, A.V. Pivovarova, I.S. Chernik, N.B. Gusev, D.I. Levitsky, Small heat shock protein Hsp27 protects myosin S1 from heat-induced aggregation, but not from thermal denaturation and ATPase inactivation, *FEBS Lett.* 582 (2008) 1407–1412.
- [35] U. Gesierich, W. Pfeil, The conformational stability of α -crystallin is rather low: calorimetric results, *FEBS Lett.* 393 (1996) 151–154.
- [36] H.A. Khanova, K.A. Markossian, S.Yu. Kleimenov, D.I. Levitsky, N.A. Chebotareva, N.V. Golub, R.A. Asryants, V.I. Muronetz, L. Saso, I.K. Yudin, K.O. Muranov, M.A. Ostrovsky, B.I. Kurganov, Effect of α -crystallin on thermal denaturation and aggregation of rabbit muscle glyceraldehyde-3-phosphate dehydrogenase, *Biophys. Chem.* 125 (2007) 521–531.
- [37] R. Stamler, G. Kappe, W. Boelens, C. Slingsby, Wrapping the α -crystallin domain fold in a chaperone assembly, *J. Mol. Biol.* 353 (2005) 68–79.
- [38] M.M. Garcia-Mira, M. Sadqi, N. Fischer, J.M. Sanchez-Ruiz, V. Munoz, Experimental identification of downhill protein folding, *Science* 298 (2002) 2191–2195.
- [39] V. Munoz, Thermodynamics and kinetics of downhill protein folding investigated with a simple statistical mechanical model, *Int. J. Quant. Chem.* 90 (2002) 1522–1528.